Catalysis Letters Vol. 111, Nos. 1–2, October 2006 (© 2006)
DOI: 10.1007/s10562-006-0123-x

Catalytic CO oxidation reaction studies on lithographically fabricated platinum nanowire arrays with different oxide supports

A. M. Contreras,[a,b,*] X.-M. Yan,[b] S. Kwon,[c] J. Bokor,[c,d] and G. A. Somorjai[a,b]

[a]*Department of Chemistry, University of California, Berkeley, CA, 94720, USA*
[b]*Materials and Chemical Sciences Divisions, Lawrence Berkeley National Laboratory, Berkeley, CA, 94720, USA*
[c]*The Molecular Foundry, Lawrence Berkeley National Laboratory, Berkeley, CA, 94720, USA*
[d]*Department of Electrical Engineering and Computer Science, University of California, Berkeley, CA, 94720, USA*

Received 5 March 2006; accepted 7 May 2006

Deep-ultraviolet lithography has been coupled with size-reduction and nanoimprint lithography to create high-density arrays of 20-nm wide platinum nanowires supported on oxide thin films of silica, alumina, zirconia, and ceria. These nanowire arrays have been used as two-dimensional platinum model catalyst systems to study the effects of support on catalytic activity during the catalytic oxidation of carbon monoxide. Strong support dependence is seen for both reaction turnover frequency and the measured activation energy. In addition, the stability of the nanowire arrays under reaction conditions shows support dependence.

KEY WORDS: CO oxidation; platinum nanowires; model catalysis.

1. Introduction

Heterogeneous catalytic reactions are of extreme importance to the chemical industries. The transition metal industrial catalysts used to carry out these reactions are very complex systems usually consisting of metal nanoparticles in the 1–100 nm size-range deposited on high surface-area supports. The particle size, surface structure and the oxide–metal interface all influence catalytic activity, selectivity, and resistance to deactivation. Model metal catalysts, usually in the form of single crystals, have been used with success to elucidate many of the atomic scale ingredients that influence catalytic performance. Single crystals, however, inherently lack the complexity of industrial catalysts, and therefore, cannot fully model the workings of these catalysts. Factors such as the oxide–metal interface [1,2] and the metal particle size [3], for instance, are known to greatly affect catalytic activity. The oxide–metal interface has previously demonstrated the ability to continue turning over reaction despite being poisoned by CO during the catalytic hydrogenation of ethylene [1,2]. The nanowire arrays described in this paper offer a system that can be used to dissect the inner workings of industrial catalysts, in that, factors such as the wire width, height and different types of support can be systematically varied to see the induced effect on catalytic activity.

The catalytic oxidation of CO to CO_2 is very important environmentally and industrially [4,5] and thus is a well studied reaction [6–9]. On Pt(111), this reaction takes place in two main temperature regimes. Below the ignition temperature, CO and O combine on the platinum surface and desorb as CO_2. The reaction follows Langmuir–Hinshelwood kinetics and the dominant surface species on platinum during reaction is CO [10]. Above the ignition temperature, SFG has shown that the surface is mainly covered by oxygen adatoms [10]. In this regime, the reaction is mass-transport limited and CO reacts with the oxygen-covered platinum surface to form CO_2 and desorb. These studies on Pt(111) have revealed surface species present during reaction above and below ignition, but as explained above, single crystals lack the oxide–metal interface present in most industrial systems. Much is still not understood about the interaction of support with the metal and the effects this interaction will have upon the metal structure to aid or hinder reaction. Support–metal interactions can change reaction kinetics by decoration of the metal surface or inducing changes in the metal structure and thus change the pathway by which the surface reaction occurs.

This report describes the fabrication of dense arrays of platinum nanowires deposited on oxide thin film surfaces of ZrO_2, SiO_2, Al_2O_3, and CeO_2. These nanowire arrays have been used to study the effects of oxide support on the catalytic oxidation of CO. The catalyst samples have been fabricated by combining lithographic nanofabrication [11] and nanoimprint technology [12,13]. The nanowire dimensions are uniform and are controllable with nanometer precision. The typical

*To whom correspondence should be addressed.

dimensions of a single platinum nanowire are 20 nm × 5 nm × 12 μm (width × height × length).

2. Experimental methods

2.1. *Pt nanowire arrays on planar oxide supports: fabrication by size-reduction lithography, and nanoimprint lithography*

The use of size-reduction lithography (SRL) to define a nanowire array of crystalline silicon has been detailed elsewhere [14–16]. This silicon nanowire array was then used to transfer its pattern to various substrates for fabrication of 2D model metal catalysts by nanoimprint lithography. The SRL process is shown schematically in figure 1. The first step of the process is thermal oxidation of the Si(100) wafer. This thermal oxide (SiO_2) is grown to a thickness of 50–70 nm. Next, a 120-nm poly-crystalline silicon (poly-Si) film is deposited by LPCVD of silane (SiH_4). A positive photoresist is spincast upon the poly-Si layer and exposed to radiation through a patterned mask. This patterning is carried out with a deep-UV (DUV) lithography stepper (ASML). The radiation-exposed polymer is then removed by a developer solution. The pattern is transferred to the underlying poly-Si substrate by reactive ion etching with HBr and Cl_2 plasma. The remaining photoresist is then removed by O_2 plasma ashing of the resist, and the pattern is left in the poly-Si layer. The pattern features are 250-nm wide, 12-μm long and have 250-nm spacing. This photolithographic patterning is followed by size-reduction lithography to reduce the pattern feature size. This is done by first conformally depositing high-temperature silicon oxide (HTO) over the poly-Si surface. As mentioned, this is a conformal deposition and therefore coats the entire surface (both tops and sidewalls of poly-Si pattern). This HTO (SiO_x) film is approximately 15-nm thick and is deposited by the LPCVD of SiH_2Cl_2 and N_2O. The HTO film is then etched back anisotropically by use of CF_4 plasma, which exposes the underlying poly-Si features. The poly-Si features are then selectively removed by etching with HBr and Cl_2 plasma. The selective removal of the poly-Si leaves the 15-nm wide sidewall form the HTO film deposition. These HTO walls can then be used as an etch mask to transfer the pattern down into the thermal oxide by etching anisotropically with CF_4 plasma, and further transferring the pattern into the Si(100) wafer by etching with HBr and Cl_2 plasma. Coupling anisotropic techniques like RIE with conformal deposition techniques like LPCVD is what allows the size-reduction to function. The minimum feature size generated by this patterning method is not limited by the photolithography pattern, but by the thickness of the conformal deposition over the photolithographically defined features. The feature spacing, however, is limited by the photolithography unless multiple cycles of the SRL are used to decrease that as well [14]. In this manner, we have batch-fabricated sub-20 nm Si wires from 250-nm patterns generated DUV photolithography (figure 2a, b).

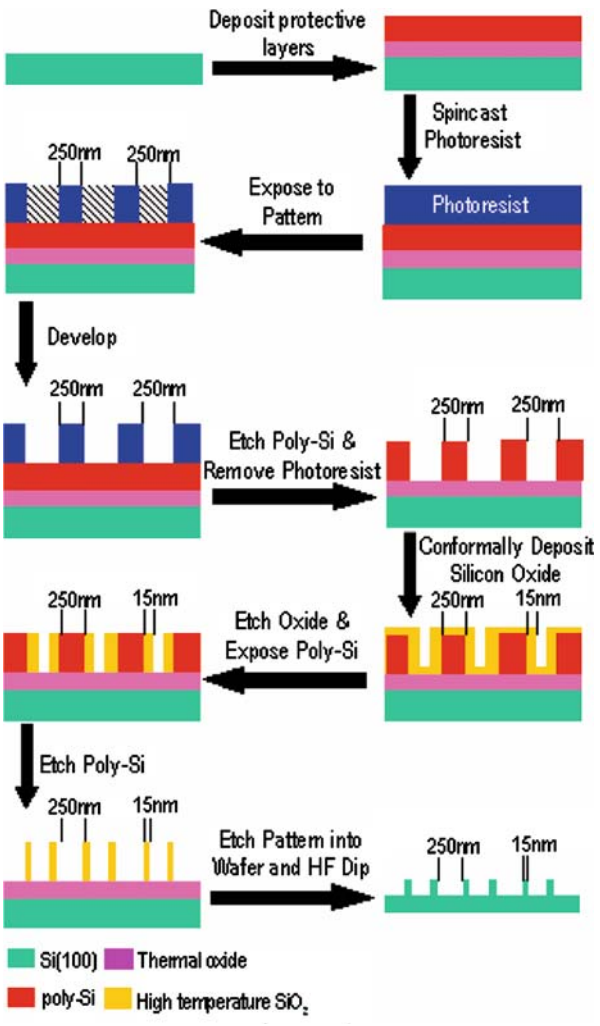

Figure 1. Schematic of the size-reduction lithography process.

The crystalline Si nanowire array fabricated by SRL is used as a mold to transfer its pattern by use of nanoimprint lithograph (NIL). NIL is a pattern transfer technique, which will be used to create our platinum nanowire arrays on different substrates. The NIL process is shown schematically in figure 3. This study focuses on the substrate effects in catalysis. Thus, zirconia, ceria, alumina, and silica thin film substrates were used as the support for the platinum nanowire arrays. The silica substrates are fabricated by oxidizing the Si(100) wafer at 1173 K in H_2O_g and O_2 until a 100-nm thin oxide film was present. Alumina, zirconia and ceria oxide films are deposited onto the Si(100) wafer (with native oxide) by electron-beam evaporation at a rate of 0.2 nm/s. The e-beam evaporator has a base-pressure 1×10^{-6}Torr and a beam collimation of ~5 mrad. After deposition, the oxides are annealed at 1173 K for 4 h under oxygen ambient. Stoichiometric Al and Zr oxides

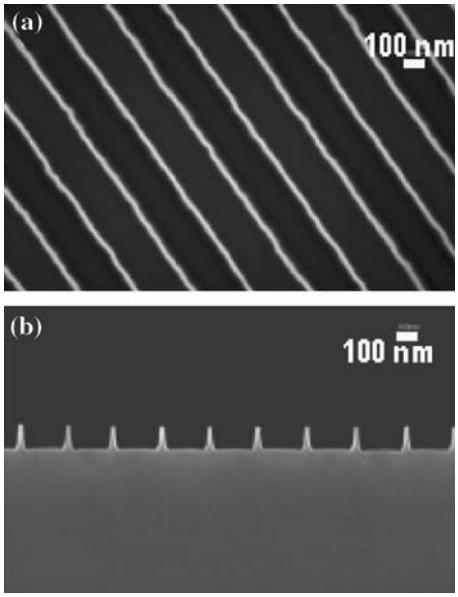

Figure 2. (a) and (b) SEM top and cross-section views of the final nanostructures, which are used as an imprint mold in nanoimprint lithography. The mold of Si wires has features of 16-nm wide and 110-nm high with 250-nm pitch. The white bar is 100 nm.

are formed after oxygen annealing, but Ce suboxide (CeO_x) is revealed by XPS [17]. The oxide thin film substrates were then used for the NIL process. Polymethylmethacrylate (PMMA) ($M_w = 15$ k) was spincast onto the oxide surface to be used as the imprint resist. The PMMA is dissolved in toluene at room temperature and left overnight to ensure full dissolution of the PMMA. The PMMA solution is 8% PMMA by mass. The solution is then filtered by use of a 0.2μm PTFE filter to remove any undissolved particles from the solution, which helps thin film uniformity when spincasting the resist. Next, the solution is ultra-sonicated for 3 h to remove any dissolved gas from the solution. The PMMA solution is spincast upon the oxide thin film substrate at 5600 rpm for approximately 30 s. This results in a PMMA film thickness of ~160 nm as checked by reflectometry. Immediately after the film is spincast, it is baked in a box furnace for 5 min at 423 K. To facilitate the separation of the mold and PMMA-coated substrate after imprinting, the surface of the Si mold is functionalized by tridecafluoro-1,1,2,2-tetrahydrooctyl-1-trichlorosilane (FTS) to form a fluorine terminated self-assembled monolayer (SAM) before use. To form the SAM layer, the mold is first cleaned in piranha solution (98% H_2SO_4 + 30% H_2O_2) at 393 K to rid the surface of any organic contamination from atmosphere. After, this cleaning procedure, the surface oxide of the mold becomes hydrogen-terminated (silanol groups). This cleaned mold is then placed into an oven filled with 2 mTorr FTS at 363 K for 300 s. Water contact angle measurements show an angle larger than 105°, which verifies that the surface is functionalized. Functionalizing the surface lowers the surface energy and allows more facile separation of the mold from the PMMA-covered substrate.

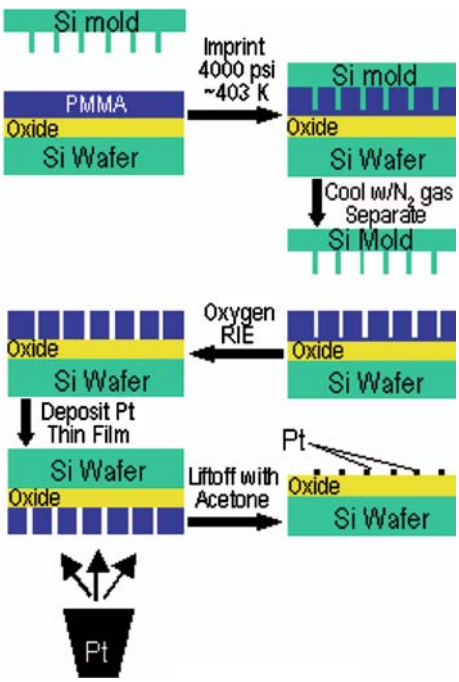

Figure 3. Schematic of the nanoimprint lithography process.

With the substrate and the mold ready for imprint, they are clipped together in a class-100 clean room to avoid any particulate contamination that may ruin the conformal contact between the mold and substrate. The samples are placed between two stainless steel plates that have been machined flat. They are then placed into a home-built hydraulic press equipped with a heating ring to heat the sample and a mechanical pump for evacuation of any gases generated during the imprint process. The sample is heated at a rate of 2 K/min by use of the resistive heating ring surrounding the imprint cell. The sample is heated to a temperature of 403 K, which is above the glass transition temperature of PMMA (PMMA $T_g = 378$ K). At 403 K, the mold is pressed into the substrate at 4000 psi for 5 min. After the imprint, the sample is cooled to room temperature by flowing a stream of nitrogen gas over the imprint apparatus. During cooling the applied pressure is maintained. After cooling to room temperature, the substrate and mold are manually separated. This leaves the negative imprint of the mold in the PMMA layer. The width of the imprinted trenches is about 2 nm larger than the dimension of the original Si wires. It is believed that the broadening is not the result of the imprinting process but the FTS SAM cover layer. As well, there is still residual PMMA on the bottom of the imprinted features. The underlying oxide surface is exposed by removing the residual PMMA by anisotropically etching with oxygen plasma. Due to an isotropic contribution to the PMMA etching, the trench width in the PMMA is increased by a few nanometers. After the residual PMMA is removed, platinum is vacuum deposited at a

rate of 0.1 nm/s by e-beam evaporation in the above described e-beam system. Pt is deposited through the imprinted features and onto the exposed oxide substrate. The remaining polymer is removed by immersing the substrate into an acetone bath and ultrasonicating for 5 min. After this polymer liftoff, the nanowire has been duplicated, and platinum nanowires are left on the surface of the various oxides prepared. This technique has been used to create 19-nm wide, 5-nm high Pt nanowire arrays on thin film oxides of silica, ceria, alumina and zirconia (figure 4a–d).

2.2. Characterization

Pt nanoarrays were characterized by scanning electron microscopy (SEM), atomic force microscopy (AFM), and X-ray photoelectron spectroscopy (XPS). SEM images are taken with a JEOL JSM-6340F equipped with a cold field emission source operating between 3 and 10 kV with a probe current of 12μA. All SEM images are acquired using an E-T combined backscatter and secondary electron detector at a working distance of 6 mm. Typical SEM images of the samples are shown in figure 4a–d. AFM is used to determine the height of the platinum features and to verify the periodicity of the arrays. AFM images (not shown) of the nanowire arrays are taken on a Park Scientific Instruments, M5 AFM. The AFM uses a feedback loop between a scan piezo and a position-sensitive photodiode array at a constant force to monitor the reflected laser light from the backside of the cantilever. XPS spectra are taken to analyze the chemical composition of the surface after fabrication and after reaction studies. Spectra are taken on a 15-kV, 40-Watt PHI 5400 ESCA/XPS system equipped with an Al anode X-ray source. Samples are cleaned of any foreign particulates before being analyzed with a stream of nitrogen gas. The spectra are inspected for the Pt $4f_{7/2}$ and $4f_{5/2}$ peaks to verify that platinum had been deposited. As well, the spectra verify the presence of the characteristic Zr, Ce, Si and Al peaks for each of the oxide substrates. For comparison of the samples before and after CO oxidation reaction, the XPS peaks were fit using XPS PEAK 4.1, which employs a least-squares fitting method. A Shirley background subtraction was used and Gauss–Lorentz peak fitting. Known powder references were used for comparison. As there was silicon migration seen through the oxide support from the silicon wafer, in some cases, and further support oxidation in other cases, Pt peak signals were compared to the signal of peaks from all elements in support (oxide support and Si signals).

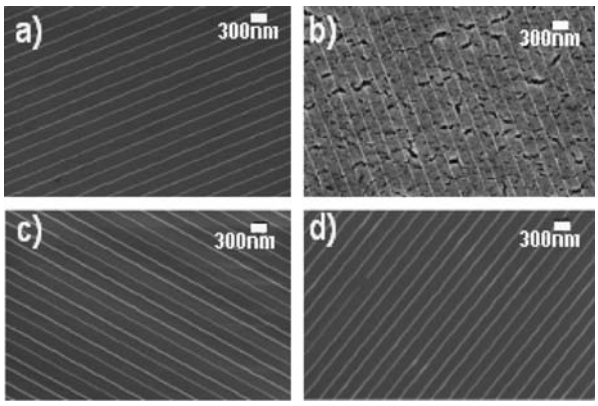

Figure 4. SEM images of 20-nm wide Pt nanowires on different oxide supports. All wires have 5-nm height. (a) silica support; (b) ceria; (c) alumina support; (d) zirconia-support.

2.3. Reaction apparatus

The reaction studies are carried out in an ultrahigh vacuum (UHV) equipped with a high-pressure cell. The general design of this type of chamber has been described elsewhere [18,19]. The outer chamber achieves a bakeout pressure of 1×10^{-10} Torr and a working pressure of 1×10^{-9}Torr between reactions. The chamber was evacuated by use of a turbomolecular pump (Balzers TPU 330), and an ion pump (Varian). The sample is mounted on a boronitride heater (Advanced ceramics, HT-01) with aluminum clips and gold-plated stainless steel screws. The sample temperature is measured with a 0.010 in. K-type thermocouple clamped to the sample with an aluminum clip and an alumina spacer. The alumina spacer is used to avoid electrical contact between the heater and the thermocouple. The sample is initially cleaned by two cycles of 1×10^{-6} Torr NO_2 at 573 K for 30 min, to oxygenate carbonaceous contaminants from the platinum surfaces, and annealed under vacuum at 1023 K for 5 min. Annealing studies performed under a helium flow showed the platinum nanowire structures to be stable at this temperature. Between reaction runs, the surface is cleaned by dosing 1×10^{-6} Torr NO_2 at 573 K for 20 min. This NO_2 treatment leaves atomic oxygen on the surface, and thus is equivalent to a pre-adsorption of oxygen onto the platinum surface. The sample cleanliness is verified by AES. All Auger spectra are taken using a Physical Electronics Industries, Inc. Auger system. As the Auger process itself can deposit carbon impurities on the surface of the sample, the sample is always cleaned after any Auger spectra are taken. Ceria supports are well known to adsorb NO_x species and are used in the catalytic converter of cars to store these emissions and help in their reduction to N_2. Post-reaction XPS measurements show no nitrogen on the surface, so any NO_x that was left on the surface in the case of the ceria-supported nanowires has desorbed. A schematic of the UHV reaction system is shown in figure 5.

2.4. Reaction studies

Every sample is cleaned as described above before introducing reaction gases. Catalytic studies are carried out on all catalyst samples using 40Torr CO, 100Torr O_2, and 620Torr He gas. Gases are premixed in the gas

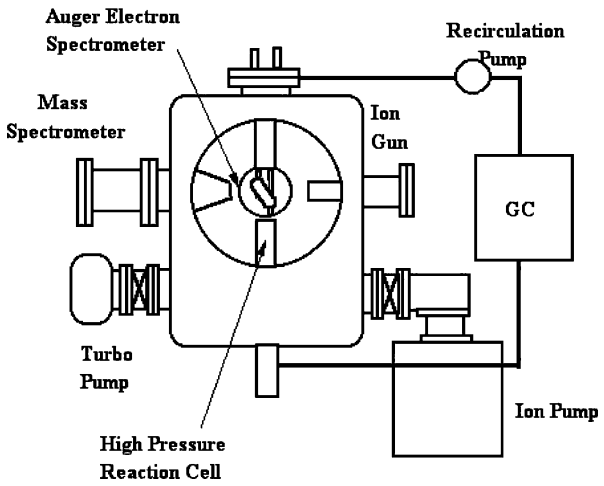

Figure 5. Schematic of reaction apparatus.

manifold approximately 20 min before introduction to the catalyst and the reaction line (during NO_2 cleaning). Upon completion of the NO_2 dosing, the reaction gases are introduced into the reaction loop. In the reaction loop, the gas mixture consists of 100Torr O_2, 40Torr CO, and 620Torr He. The purities of O_2, CO, and He gases used in reaction studies are 99.997, 99.99, and 99.9999%, respectively. All gases are used as received from Airgas without further purification. The gases are circulated through the reaction line by used of a Metal Bellows recirculation pump at a rate of 2 L/min. The volume of the reaction loop is 0.225 L. A HP Series II gas chromatograph (GC) equipped with a TCD detector and a 15' × 1/8" SS 60/80 Carboxen-1000 (Supelco) is used to separate the products for analysis. The GC is part of the reaction loop and samples the circulating reaction gases every 5 min by use of a 6-port automatic sampling valve. The measured reaction rates are reported as turnover frequencies (TOF) and are measured in units of product molecules of CO_2 produced per platinum surface site per second of reaction time. The number of platinum sites is calculated by geometrical considerations. The nanowires walls are considered to be rectangular and standing upright on a planar support. By using SEM measurements to calculate the surface area of a wire and dividing by the surface density of platinum, the number of surface platinum sites available for reaction is calculated.

3. Results

3.1. Nanowire samples on zirconia, ceria, alumina, and silica

SEM images of the nanowire arrays on the different oxides show the nanowire diameters to be 19 ± 2 nm for the zirconia, ceria and silica supported samples and 20 ± 2 nm for the alumina-supported samples. SEM measurements also show the distance in the middle of the wire to be 250 ± 2 nm between two different wires to be 248 ± 3 nm. AFM images of the nanowires, show them to have a height of 5 ± 1 nm (not shown) and confirm the width of the Pt features. SEM images of the nanowire arrays are shown in figure 4a–d

3.2. CO oxidation reaction studies

Catalytic oxidation of CO to CO_2 over the various catalyst arrays was carried out in the 513–613 K temperature range, which is above the ignition temperature. Above the ignition temperature, the reaction rate is mass-transport limited. For this reason, the measured activation energies will be compared to the literature rather than the measured turnover frequencies (TOF) of reaction, because different flow rates and reactor volumes can change the turnover rate measured for a given system. However, the reaction turnover for all arrays are discussed in general and compared to gauge the reactivity of all supported arrays in comparison to one another. A summary of the measured activation energies is shown in table 1 for all of the supported catalysts. These values are shown in comparison to Pt(111) [10,20] and a 15-nm Pt thin film deposited onto a Si(100) wafer with native oxide. A typical CO_2 accumulation curve is shown in figure 6. The accumulation curves yield the rate of reaction at different temperatures and using this information, Arrhenius plots are constructed to obtain the apparent activation energy of reaction. The Arrhe-

Table 1
Summary of measured activation energies for CO oxidation.

Catalyst	E_a(kcal/mol)
Pt(111)	14 (A.l) & 42 (B.l)
15-nm Pt thin film on Si(100) water	13.7 ± 0.4 (A.l)
	26.9 ± 0.1 (B.l)
Nanowires on SiO_2	15.9 ± 0.6
No Annealing	
Nanowires on SiO_2	12.6 ± 0.2
Annealing at 1023 K	
Nanowires on CeO_2	18.8 ± 0.2
Nanowires on Al_2O_3	17.1 ± 0.4
Nanowires on ZrO_2	14.6 ± 0.2

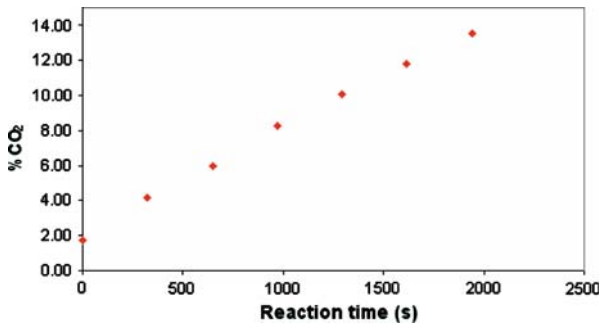

Figure 6. CO_2 accumulation curve measured on a zirconia-supported platinum nanowire array at 553 K.

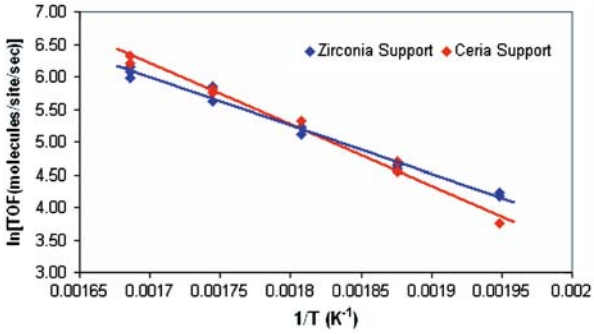

Figure 7. Arrhenius plots measured for CO oxidation reactions on zirconia and ceria-supported Pt nanowire arrays.

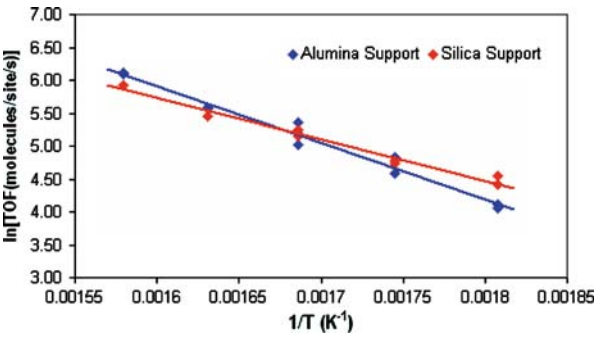

Figure 8. Arrhenius plots measured for CO oxidation reactions on alumina and silica-supported Pt nanowire arrays.

nius plots for reaction on the zirconia and ceria-supported samples is shown in figure 7 and the Arrhenius plots for the alumina and the silica-supported samples are shown in figure 8. The Arrhenius plots for reaction on the 15-nm Pt film on silicon is shown in figure 9.

The apparent activation energy for the Pt(111) single crystal and the 15-nm Pt film on silicon, which were used as reference states of platinum, are 14 kcal/mol [10] and 13.7 ± 0.4 kcal/mol, respectively. The Pt thin film is also used to measure the activation energy below ignition, which was measured to be 26.9 ± 0.1 kcal/mol. Apparent activation energies for the zirconia and ceria-supported wire arrays are 14.6 ± 0.2 kcal/mol and 18.8 ± 0.2 kcal/mol, respectively. The nanowires on silica have an activation energy of 12.6 ± 0.2 kcal/mol.

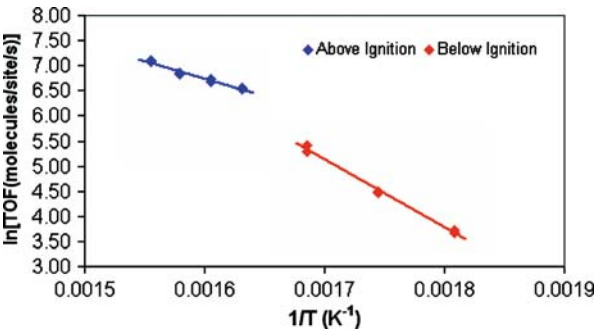

Figure 9. Arrhenius plots measured for CO oxidation reactions on a 15-nm platinum film supported on a Si(100) wafer.

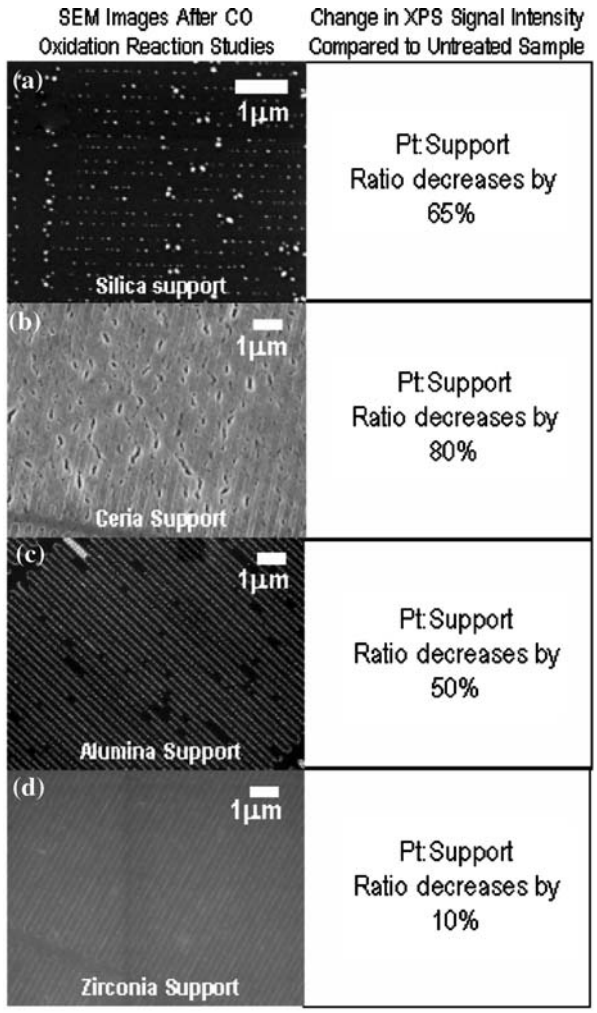

Figure 10. Post-reaction analysis of Pt nanowire samples (Right) SEM images (Left) Changes measured in Pt by XPS (a) Silica-support; (b) ceria-support; (c) alumina-support; (d) zirconia-support.

The apparent activation energy measured on the alumina-supported sample is 17.1 ± 0.4 kcal/mol.

After CO oxidation, SEM images are taken *ex situ*, to monitor any change of the nanowire morphology (left side of figure 10a–d). The zirconia and ceria-supported wires are both stable under for the cleaning and reaction studies (figure 10b, d, respectively). The silica sample is no longer a nanowire but particles of various sizes as the surface tension of platinum on silica was enough to cause particle formation on the surface (figure 10a). The alumina-supported sample while it did form particles stays in a wire form as shown in figure 10c.

As well, post-reaction XPS spectra are taken *ex situ* to observe any differences in the Pt:support signal ratio. These results are also summarized in figure 10a–d (right side). On the silica-supported sample, a decrease of 65% in the Pt:support signal ratio is measured (figure 10a). The ceria-supported nanowire array shows an 80% decrease in the Pt:support ratio after reaction (figure 10b). The alumina-supported wires also see a

large decrease with a decrease of 50% of the Pt:support signal ratio (figure 10c). There is a 10% decrease is the Pt 4f signal measured for the zirconia-supported Pt wires (figure 10d).

The relative turnover frequencies measured for the four different arrays showed a definite trend for the different arrays as shown below.

$$\textit{Pt array support trend seen in TOF } (573\,K):$$
$$\textit{Silica} < \textit{Alumina Zirconia} < \textit{Ceria}$$

The ceria-supported Pt array had a turnover more than triple that of the silica and alumina-supported arrays and about 50% more than that of the zirconia-supported array.

4. Discussion

4.1. CO oxidation reaction studies

The apparent activation energy above ignition on the Pt thin film compares well with that of the Pt(111) single crystal. Measurement of CO oxidation over the Pt thin film shows two different reaction regimes. Above ignition, the apparent activation energy is measured at about 14 kcal/mol, which is essentially the same as that measured for the Pt(111) single crystal. Below ignition, the apparent activation energy measured for the Pt thin film was about 27 kcal/mol, with ignition occurring between 593 and 613 K. The nanowire arrays are as well Pt thin films deposited in the same manner (electron beam evaporation), except that they are formed into structures on the planar oxide surface. This provides the nanowires with an oxide–metal interface, which adds an additional ingredient to affect reactivity.

The apparent activation energy measured for the silica-supported array was about 13 kcal/mol, which compares well to the 14 kcal/mol measured for the thin film and single crystal. SEM images after reaction show that the platinum wires have broken and balled up on the oxide surface (figure 10b), and XPS shows a decrease of the Pt 4f signal of 65%. This can be due to several factors such as the platinum breaking up and minimizing its surface area, or the migration of platinum into the support. Figure 10b clearly shows that the platinum balls up and loses its wire structure on the support. As well, platinum is known to wet the silica surface and migrate into the support as shown by Yu *et al.* [21]. In an oxygen environment, the diffusion coefficient for oxygen through silica is orders of magnitude greater than the diffusion coefficient of silicon through silica [22]. So, if silicides are formed, they must be formed with silica and not the pure silicon migrating through the silica support. Thus, the 65% loss in the Pt signal is due to a combination of the platinum reducing its surface area by balling up on the silica and migrating into the support. It is interesting that these nanowires formed particles on the silica surface, because annealing studies in He for 2 h at 973 K showed them to break up in parts, but they did not ball up to form particles. There were only very slight breaks in the wires. Thus, the oxygen ambient facilitates platinum mobility on the silica surface.

The apparent activation energy for the ceria-supported nanowire arrays is about 19 kcal/mol, which is higher than both the platinum thin film and single crystal. This is however comparable to other ceria-supported arrays [23,24], which show apparent activation energies anywhere from 8–21 kcal/mol. The wire structures on this sample remained stable despite the annealing and reaction conditions (figure 10c). XPS, however indicates an 80% decrease in Pt signal after reaction in comparison to before. Despite this drop in signal, though, the ceria-supported Pt wires have over double the turnover frequency of the silica and alumina-supported wires. Hardacre *et al.* have seen that depositing ceria on Pt(111) with different coverages can change the turnover frequency of reaction for CO oxidation and the activation energy [23]. It has also been shown that the oxide-covered metal can turnover just as much and sometimes more than the metal on its own. Since there is a drop in the platinum signal seen by XPS after annealing and reaction, the platinum wires are most likely decorated by the ceria and continuing to turnover reaction by some Pt/Ce species or Pt/CeO_x species. While still active as reaction sites, this type of compound may make it more difficult for reactants to reach metal sites for dissociation and desorb as products. The reaction rate, however, seems to be enhanced, which can be attributed to the ability of ceria to accept and donate oxygen atoms during reaction [25–28]. Figure 11 shows the XPS spectra of the ceria-supported samples before and after reaction. Figure 11a, which shows the Pt 4f peaks before and after reaction, is typical of the samples that lose platinum after reaction. Figure 11b shows two peaks fitted to the spectrum in the O1s binding energy area. The lower binding energy peak is assigned to the ceria support oxygen. This does shift after reaction, which is indicative of less oxygen content in the oxide [29]. The higher binding energy peak is assigned to the $O^{\delta-}$ peak associated with carbonate groups from the binding of CO and CO_2 to the ceria surface from atmosphere and during reaction [23,30].

The apparent activation measured on the alumina-supported array was 17.1 kcal/mol. This is 3 kcal/mol higher than for the Pt(111) single crystal and thin film. However, it is considerably lower than other values seen for Pt/Al_2O_3 ranging from 26 to 41 kcal/mol [24,31]. It has been seen that the apparent activation energy is sensitive to the structure of the alumina onto which the Pt is deposited [31]. The reaction conditions appear to cause the Pt wires to break and create Pt particles (figure 10d). Post-reaction XPS measurements show a 50% decrease in the Pt 4f signal. This decrease in the Pt surface area is similar to that of the silica-supported case in that the decrease is most likely caused by the balling

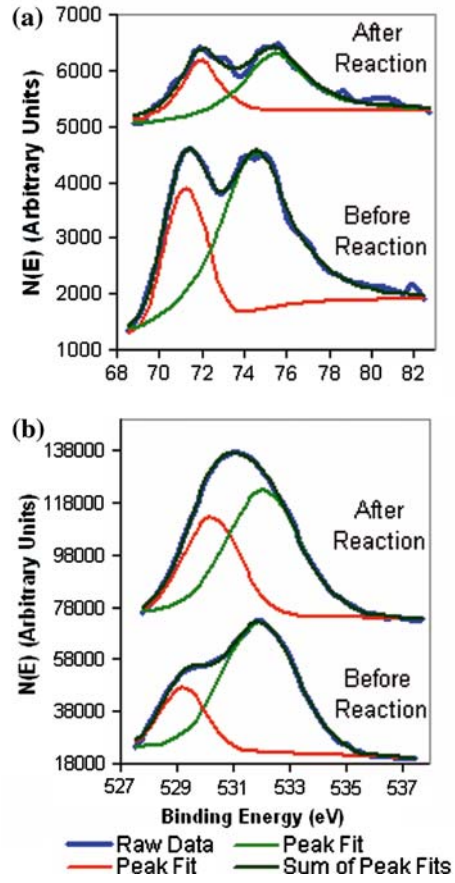

Figure 11. XPS characterization of the ceria-supported Pt nanowire array (a) Pt 4f peaks before and after reaction showing loss of surface platinum (b) O1s peaks before and after CO oxidation reaction showing the O^- of the carbonate groups from CO and CO_2 groups binding to the ceria surface.

up of the Pt and the migration of the Pt into the support [32]. As well, there is a 90% increase in the Si to Al peak ratio after reaction, which means that there is significant Si migration through the alumina support. Thus, there could also be platinum silicides forming, which are not catalytically active and would reduce the number of active metallic sites available for reaction.

CO oxidation measured on the zirconia-supported nanowire array gives an apparent activation energy of about 14.6 kcal/mol, which is very close to the values measured on the Pt single crystal and thin film. The nanowire structures seem to be stable after annealing at 1023 K in vacuum and the reaction studies (figure 10e). Post-reaction XPS measurements show the Pt signal decrease by 10% and the Si to Zr peak ratio increase by 50%. The fact that the Pt signal does not decrease significantly is the most likely reason that this array has as high of a turnover frequency as the ceria support.

The support trend for measured reaction turnover is shown above. The ceria and zirconia-supported arrays have the highest turnover rates of the four arrays, and of these two arrays ceria turns over about 50% more. It is believed that the reason the zirconia-supported array has such a high TOF is due to the stability of platinum throughout the reaction studies. The ceria-supported array shows a similar TOF to the zirconia-supported array, but has an 80% decrease in the amount of surface platinum. Thus, the TOF is likely due to the strong metal–support interaction of the ceria-decorated platinum surface. Both the alumina and silica-supported arrays had lower turnover and showed significant decrease in the platinum signal. In both arrays, there is the possibility of platinum migrating into the support, which is the likely cause of the lower turnover. As well, there may be silicides forming on both of these arrays since Si migration was seen in the alumina-supported array. This platinum would show up in the XPS measurements, but would not be catalytically active.

The use of lithography for fabrication of two-dimensional nanoarrays as model catalysts offers the opportunity to change different aspects about the catalyst while holding all other features the same. These investigations into the reaction kinetics of CO oxidation and platinum nanowire array stability indicate that reaction rates, activation energies, and structural stability have a large support dependence. Future work with such well-defined systems can be furthered by controlling diffusion through the oxide supports and using single-crystalline oxide surfaces to help further unravel the importance of the support–metal interactions. Model catalyst systems allow a deeper understanding of the pertinent surface chemistry occurring during catalytic reaction and will therefore help further the cause of perhaps one day being able to tune a catalyst to the specific reaction for which it will be used.

5. Conclusions

DUV has been coupled with NIL to produce sub-20 nm platinum nanowire arrays on oxide supports of silica, alumina, ceria and zirconia. These two-dimensional model catalyst arrays have been used to study the support dependence of CO oxidation reaction kinetics and indicate that the most important factor affecting turnover frequency is the interaction of the platinum and the support, while the activation energy is most heavily affected by clean platinum being on the surface of the oxide. Further studies with oxide supports of controlled surface structure can help to balance these two factors and truly tune the catalyst to the reaction.

Acknowledgments

This research was supported by the Director, Office of Energy Research Office of Basic Energy Sciences, Chemical and Materials Sciences Divisions, of the US Department of Energy under Contract No. DE-AC02-05CH11231.

References

[1] A.M. Contreras, J. Grunes, X.-M. Yan, A. Liddle and G.A. Somorjai, Catal. Lett. 100 (2005) 115.
[2] J. Grunes, J. Zhu, E.A. Anderson and G.A. Somorjai, J. Phys. Chem B 106 (2002) 11463.
[3] M. Valden, X. Lai and D.W. Goodman, Science 281 (1998) 1647.
[4] J.T. Kummer, J. Phys. Chem. 90 (1986) 4747.
[5] C.H.F. Peden, D.W. Goodman, D.S. Blair, P.J. Berlowitz, G.B. Fisher and S.H. Oh, J. Phys. Chem. 92 (1563) 1988.
[6] N.W. Cant, P.C. Hicks and B.S. Lennon, J. Catal. 54 (1978) 372.
[7] N.W. Cant and D.E. Angove, J. Catal. 97 (1986) 36.
[8] J.T. Kiss and R.D. Gonzalez, J. Phys. Chem. 88 (1984) 892.
[9] J.T. Kiss and R.D. Gonzalez, J. Phys. Chem. 88 (1984) 898.
[10] K.R. McCrea, J.S. Parker and G.A. Somorjai, J. Phys. Chem. B. 106 (2002) 10854.
[11] B.D. Gates, Q. Xu, J.C. Love, D.B. Wolfe and G.M. Whitesides, Annu. Rev. Mater. Res. 34 (2004) 339.
[12] S.Y. Chou, P.R. Krauss and P.J. Renstrom, Science 272 (1996) 85.
[13] L.J. Guo, J. Phys. D: Appl. Phys. 37 (2004) R123.
[14] Y.K. Choi, J.S. Lee, J. Zhu, G.A. Somorjai, L.P. Lee and J. Bokor, J. Vac. Sci. Tech. B 21 (2003) 2951.
[15] Y.K. Choi, J. Zhu, J. Grunes, J. Bokor and G.A. Somorjai, J. Phys. Chem. B 107 (2003) 3340.
[16] X.-M. Yan, S. Kwon, A.M. Contreras, J. Bokor and G.A. Somorjai, Nano Lett. 4 (2005) 745.
[17] X.-M. Yan, S. Kwon, A.M. Contreras, M.M. Koebel, J. Bokor and G.A. Somorjai, Catal. Lett. 105 (2005) 127.
[18] J.C. Schlatter and M. Boudart, J. Catal. 24 (1972) 482.
[19] E. Segal, R.J. Madon and M. Boudart, J. Catal. 52 (1978) 45.
[20] X. Su, P.S. Cremer, Y.R. Shen and G.A. Somorjai, J. Am. Chem. Soc. 119 (1997) 3994.
[21] R. Yu, H. Song, X.-F. Zhang and P. Yang, J. Phys. Chem. B 109 (2005) 6940.
[22] M.J. Madou, *Fundamentals of Microfabrication: The Science of Miniaturization* 2 ed.(CRC Press, New York, 2002).
[23] C. Hardacre, R.M. Ormerod and R.M. Lambert, J. Phys. Chem 98 (1994) 10901.
[24] U. Oran and D. Uner, Appl. Cat. B 54 (2004) 183.
[25] Y.-F. Yao, J. Catal 87 (1984) 152.
[26] J.Z. Shyu, K. Otto, W.L.H. Watkins, G.W. Graham, R.K. Belitz and H.S. Gandhi, J. Catal. 114 (1988) 23.
[27] J.Z. Shyu and K. Otto, J. Catal. 115 (1989) 16.
[28] R.F. Hicks, C. Rigano and B. Pang, Catal. Lett. 6 (1990) 271.
[29] G. Praline, B.E. Koel, R.L. Hance, H.-I. Lee and J.M. White, J. Elect. Spect. Rel. Phen. 21 (1980) 17.
[30] L. Osterlund, S. Kielbassa, C. Werdinius and B. Kasemo, J. Catal. 215 (2003) 94.
[31] G.S. Zafiris and R.J. Gorte, J. Catal. 140 (1993) 418.
[32] J. Libuda, M. Baumer and H.-J. Freund, J. Vac. Technol. A 12 (1994) 2259.
[33] F. Dong, A. Suda, T. Tanabe, Y. Nagai, H. Sobukawa, H. Shinjoh, M. Sugiura, C. Descorme and D. Duprez, Catal. Today 93–95 (2004) 827.